FEATURE ARTICLE

Toward an Accurate and Efficient Semiclassical Surface Hopping Procedure for Nonadiabatic Problems

Michael F. Herman

Department of Chemistry, Tulane University, New Orleans, Louisiana 70118

Received: May 20, 2005

The derivation of a semiclassical surface hopping procedure from a formally exact solution of the Schrodinger equation is discussed. The fact that the derivation proceeds from an exact solution guarantees that all phase terms are completely and accurately included. Numerical evidence shows the method to be highly accurate. A Monte Carlo implementation of this method is considered, and recent work to significantly improve the statistical accuracy of the Monte Carlo approach is discussed.

I. Introduction

Quantum mechanical effects can play an important role in the dynamics of molecular systems. However, the numerical applications of quantum mechanics to dynamical problems are feasible only for systems with a small number of degrees of freedom. Semiclassical methods[1−12] provide a computationally attractive approximation to fully quantum calculations, because they use information obtained from classical trajectories to construct approximate quantum wave functions, correlation functions, and transition probabilities.

The coordinates in molecular systems are commonly divided into a fast set **r** and a slow set **R**. The fast set usually contains the electronic coordinates, and the coordinates of the nuclei, **R**, make up the slow set. In the Born−Oppenheimer (BO) or adiabatic approximation, the wave functions and energies for the fast subsystem are evaluated at fixed values for the slow degrees of freedom.[13] The BO Schrodinger equation is

$$\mathbf{H}^{\mathrm{f}}\varphi_n(\mathbf{r};\mathbf{R}) = E_n^{\mathrm{f}}(\mathbf{R})\,\varphi_n(\mathbf{r}'\mathbf{R}) \tag{1}$$

The Hamiltonian $\mathbf{H}^{\mathrm{f}}$ is the sum of the kinetic energy for the fast degrees of freedom, $\mathbf{T}^{\mathrm{f}}$, and the potential energy for the system $V(\mathbf{r},\mathbf{R})$. Within the BO approximation, the energy $E_n^{\mathrm{f}}(\mathbf{R})$ serves as the potential energy $W_n(\mathbf{R})$ for the nuclear motion, and the slow system Hamiltonian $\mathbf{H}^{\mathrm{s}} = \mathbf{T}^{\mathrm{s}} + W_n(\mathbf{R})$ governs the motion of the nuclei, where $\mathbf{T}^{\mathrm{s}}$ is the slow variable kinetic energy operator.

Semiclassical methods[1−12] are widely used in modeling physical systems of experimental interest when only one BO electronic state is important. However, many important processes in experimental systems involve transitions between BO states. A variety of semiclassical methods have been proposed for handling nonadiabatic transitions between BO states.[14−54] These approaches often describe the electronic wave function as a linear combination of the BO states,

$$\Psi^{\mathrm{f}}(\mathbf{r},\mathbf{R},t) = \sum_n c_n(t)\,\varphi_n(\mathbf{r},\mathbf{R}) \tag{2}$$

One approach is to evaluate $c_j(t)$ using the time dependent Schrodinger equation for the fast degrees of freedom as the slow degrees of freedom travel along classical trajectories calculated using the Hellmann−Feynman force, $\mathbf{F} = -\langle\Psi^{\mathrm{f}}|\partial\mathbf{H}^{\mathrm{f}}/\partial\mathbf{R}|\Psi^{\mathrm{f}}\rangle$, where $\langle ...\rangle$ indicates integration over **r**.[14−18] Other approaches, which are referred to as surface hopping procedures, allow the trajectories employed in the construction of the semiclassical wave functions and/or transition probabilities to take abrupt hops from one adiabatic energy surface to another.[19−42] Other methods express the coefficients in eq 2 as $c_j(t) = [n_j(t)]^{1/2}\exp[-iq_j(t)]$ and treat $n_j(t)$ and $q_j(t)$ as canonically conjugate action/angle variables that are added to the phase space of the slow coordinates **R** and momenta **P**. Classical trajectories are run in this enlarged phase space, and semiclassical wave functions and/or transition probabilities are constructed.[43−46]

In this article, we focus on work in our group using a semiclassical surface hopping approach.[22−25] The derivation of a formally exact solution to the nonadiabatic time independent Schrodinger equation (TISE) is discussed in section II. The phase and prefactor associated with each term in this wave function expansion have the form expected for semiclassical wave functions, and each term corresponds to an integration over trajectories with a certain number of hops between quantum states. This wave function expansion can be generalized for multidimensional systems and for time dependent problems as a semiclassical approximation. The important feature in this semiclassical development is the careful treatment of the phases of all the terms, which are obtained starting from the formally exact solution to the Schrodinger equation. This guarantees that all phases are treated exactly and phase interference between contributions from different trajectories is handled accurately.

The surface hopping expansions developed for the wave function and the time dependent propagator are "primitive" wave functions and propagators, because their semiclassical prefactors diverge at caustic points along the classical trajectories. Corresponding uniform versions of these surface hopping expansions, which do not have these divergences, are also discussed. The uniform propagator is an initial value representation (IVR), because it is expressed as an integration over all possible initial phase space points for the surface hopping trajectories. An IVR has the advantage that it avoids the difficult search required by the double ended boundary condition that must be satisfied by the trajectories contributing to the primitive propagator.

In section III, the Monte Carlo implementations of these surface hopping procedures are discussed. The Monte Carlo

10.1021/jp052652l CCC: $30.25
Published on Web 09/28/2005

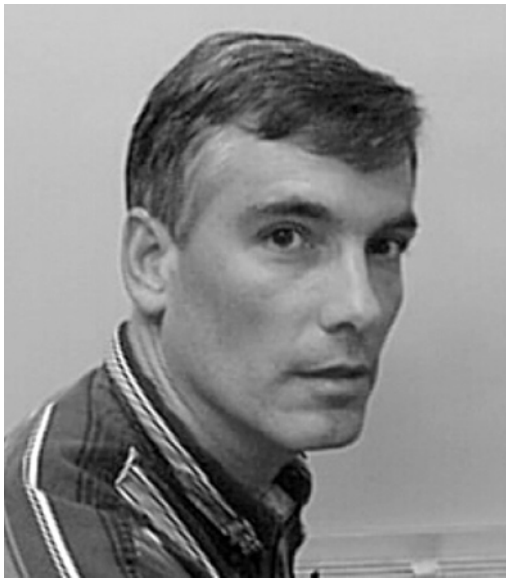

Michael Herman is a Professor of Chemistry and Dean of the Graduate School at Tulane University. After receiving his BA in biochemistry from Canisius College in Buffalo, NY, in 1975, he was an NSF graduate fellow in the Department of Chemistry at the University of Chicago. His doctoral research with Karl Freed investigated improved methods for the calculation of ionization potentials of molecules. From 1979 to 1981 Professor Herman conducted postdoctoral research with Bruce Berne at Columbia University on theoretical methods for the study of quantum effects in condensed phases. He has been a member of the chemistry faculty at Tulane since 1981, and he was selected as a Fellow of the American Physical Society in 2001. His research at Tulane has primarily focused on the development of semiclassical methods for the study of quantum processes in the gas phase and in condensed phase systems.

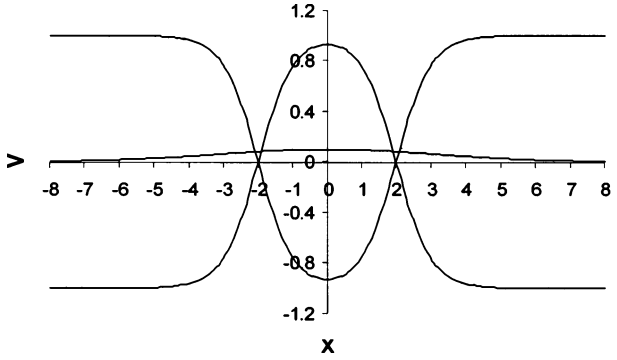

Figure 1. Diabatic potential energy surfaces for a model curve crossing problems are plotted. The potential surfaces are given by $V_{11} = -V_{22} = -\tanh(X - 2)\tanh(X + 2)$ and $V_{12} = 0.1\exp(-X^2/20)$.

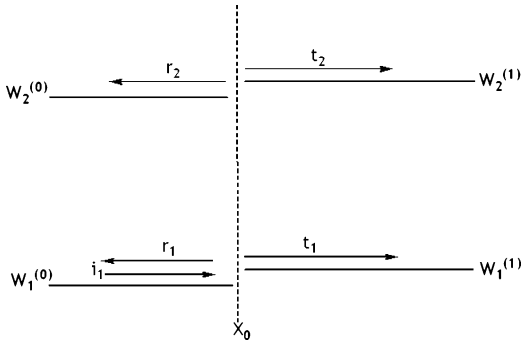

Figure 2. Incoming wave function, denoted by the arrow pointing toward X_0, is split by the discontinuity at X_0 into four outgoing wave functions, denoted by the arrows pointing away from X_0. The two transmitted (reflected) outgoing wave functions are labeled t_1 and t_2 (r_1 and r_2), corresponding to the potential surfaces W_1 and W_2.

procedure assigns a probability for hopping or not hopping for each step along the trajectory and chooses between these options. Methods for improving the statistical convergence of the Monte Carlo procedure are considered. Step probabilities are developed that include the effects of multiple hops within the step. This allows for the use of larger steps, results in fewer hopping trajectories, and reduces the interference between these trajectories. Another method for the improvement of the Monte Carlo procedure utilizes the flexibility in the choice of the representation for the quantum states of the fast subsystem to reduce the integrated coupling between the states, thereby reducing the importance of multihop trajectories. Tests of these methods are discussed. It is found that the surface hopping method is extremely accurate and that the use of these procedures results in a large reduction in the computational time required for a given level of statistical accuracy.

II. Semiclassical Surface Hopping Method

We begin with a derivation of a formally exact solution to the one-dimensional multistate time independent Schrodinger equation (TISE). For simplicity, the development here is limited to the two state case. The system can be defined in the diabatic representation by the two state energies, $V_{11}^{d}(X)$ and $V_{22}^{d}(X)$, and the diabatic coupling, $V_{12}^{d}(X)$, where X is the variable for the slow subsystem. The quantum states for the fast subsystem in the adiabatic representation are given the terms of diabatic states, φ_1^{d} and φ_2^{d},

$$\begin{pmatrix}\varphi_1(x)\\ \varphi_2(x)\end{pmatrix} = \begin{pmatrix}\cos\theta & \sin\theta\\ -\sin\theta & \cos\theta\end{pmatrix}\begin{pmatrix}\varphi_1^{d}\\ \varphi_2^{d}\end{pmatrix} \tag{3}$$

where the diabatic states, φ_1^{d} and φ_2^{d}, are taken to be independent of X and the value of $\theta(X)$ is determined by the condition that the potential energy matrix is diagonal in the adiabatic or BO representation. The elements of this diagonal matrix, $W_1(X)$ and $W_2(X)$, are the adiabatic state energies, and $W_i(X)$ serves as the potential energy for the motion of the slow coordinate when the system is in adiabatic state φ_i. Figure 1 shows $V_{11}^{d}(X)$, $V_{22}^{d}(X)$, and $V_{12}^{d}(X)$ for a model curve crossing problem. Suppose that a particle is traveling on surface W_1 in the positive direction from large negative values of X with energy E. The particle can leave the interaction region traveling in either direction on either surface. We are interested in evaluating the wave function for this system and the probability of each of these four possible outcomes.

This problem can be replaced by a piecewise constant problem[22] by partitioning the X-axis into intervals of width ΔX, with $X_0, X_1, ..., X_N$ labeling the interval boundaries, and replacing $W_1(X)$, $W_2(X)$, and $\theta(X)$ with constant values in each interval and for $X < X_0$ and $X > X_N$. This results in discontinuities in W_1, W_2, and θ at each X_j. The incoming particle on W_1 with mass m and energy E is described by the wave function $\varphi_1 \exp(ik_1X)$, where $k_j = P_j/\hbar$ and $P_j = [2m(E - W_j)]^{1/2}$. When this incoming wave function encounters the discontinuity in W_1, W_2, and θ at X_0, it splits into four particle fluxes moving away from X_0. These four fluxes correspond to reflected fluxes on each of the two surfaces and transmitted (into the next interval) fluxes on each of the two surfaces, as described in Figure 2. These fluxes are each described by wave functions of the type $\varphi_j C_j^{(\pm)} \exp(\pm ik_jX)$, where $+$ $(-)$ is used for the transmitted (reflected) flux. The $C_j^{(\pm)}$ are determined by the requirement that the wave function and its derivative must be continuous at the discontinuity.[22] Each transmitted flux travels across the next interval until

it reaches the discontinuity at X_1. At this point, it splits into two transmitted and two reflected fluxes, and the coefficient $C_j^{(\pm)}$ for each new flux is obtained as before. These new fluxes then travel across intervals and are split into four new fluxes when the next discontinuity is encountered, and so on. The sum of all possible contributions of this sort at a point X on surface W_j gives the value of the wave function in that state at X. This wave function satisfies the TISE for the piecewise constant problem. As the width of the partition of the X axis is made smaller, this wave function approaches the exact solution to the original problem with continuous $W_1(X)$, $W_2(X)$, and $\theta(X)$.[22]

In the piecewise constant problem, the reflection and transmission coefficients, $C_j^{(\pm)}$, depend on the values of θ, P_1, and P_2 on both sides of the interval boundary. In the limit of small ΔX, the coefficient for transmission with no change in adiabatic state is zeroth order in the small changes across the boundary, $\Delta\theta$, ΔP_1, and ΔP_2, whereas the coefficients for transmission with a hop to the other adiabatic state and for reflection onto either adiabatic state are first order in $\Delta\theta$, ΔP_1, and ΔP_2. For this reason, transmissions with hop and all reflections are considered first-order events, and a path with n first-order events is considered an nth-order path. The zeroth-order path, corresponding to transmission without hop at each boundary, gives rise to the contribution[22] $\psi_0 = \varphi_1\psi_{w1}(X_i,X)$ in the $\Delta X \rightarrow 0$ limit where $\psi_{w1}(X_i,X)$ is the semiclassical WKB wave function for the potential W_1(X)

$$\psi_{wj}(X_i,X) = \sqrt{\frac{P_j(X_i)}{P_j(X)}}\exp\left[\frac{i}{\hbar}\int_{X_i}^{X} P_j(X_1)\,dx_1\right] \qquad (4)$$

and X_i is an arbitrary point in the incoming asymptotic ($X \ll 0$) region.

The contribution from all first-order paths with a transmission with hop at one discontinuity, X_j (and transmission with no hop at all other boundaries) is obtained by summing over the different X_j. In the $\Delta X \rightarrow 0$ limit, this sum becomes an integration over the position of hop, and this contribution is given by

$$\psi_T = \varphi_2\int_{X_i}^{X}\tau_{12}(X_1)A_T e^{iS_T/\hbar}\,dX_1 \qquad (5)$$

$A_T = [P_1(X_i)/P_2(X)]^{1/2}$ is the WKB prefactor for the trajectory that travels on initial adiabatic surface, W_1, from X_i to X_1, hops to W_2 at X_1, and then travels from X_1 to X on W_2, and S_T is the WKB phase function for this hopping trajectory,

$$S_T = \int_{X_i}^{X_1} P_1(y)\,dy + \int_{X_1}^{X} P_2(y)\,dy \qquad (6)$$

The transmission coefficient in eq 5 is given by

$$\tau_{12} = -\frac{(P_1 + P_2)}{2(P_1P_2)^{1/2}}\frac{d\theta}{dX} \qquad (7)$$

The contribution from all paths with a single reflection with no hop and the contribution from all paths with a single reflection with a hop are obtained analogously to eq 5.

The contributions from all higher order paths can also be obtained in this manner. The contribution from all paths with two transmission with hop events is given by

$$\psi_{TT} = \varphi_1\int_{X_i}^{X}dX_1\int_{X_1}^{X}dX_2\,\tau_{12}(X_1)\,\tau_{21}(X_2)\,A_{TT}e^{iS_{TT}/\hbar} \qquad (8)$$

where $\tau_{21} = -\tau_{12}$. The prefactor A_{TT} and phase function S_{TT} are again given by WKB-like expressions for the trajectory that hops from W_1 to W_2 at X_1 and from W_2 to W_1 at X_2. The contribution with any sequence of any number of nonclassical events is obtained in the same way. The generalization of the two state case to any number of quantum states is straightforward.[22] The expansion obtained by summing all contributions of this type is a formally *exact* solution of the multistate TISE in one dimension.

The reflection without hop terms, which are independent of the nonadiabatic coupling, provide corrections to the semiclassical approximation. If all terms containing reflections without hops are neglected in the wave function expansion, then the resulting wave function satisfies the Schrodinger equation to all orders in the nonadiabatic coupling and to the same (first) order in $\hbar$ as is the case with the WKB wave function for the single surface problem.[23] Because the surface hopping expansion, including reflections without hops, provides the exact quantum wave function, the semiclassical approximation obtained by neglecting reflection without hop terms incorporates the complete and correct phase and amplitude for every possible trajectory. This is important, because many surface hopping procedures fail to accurately account for all phase interference effects.

This semiclassical surface hopping expansion can be generalized for multidimensional problems.[23] In multidimensional case, the nonadiabatic coupling $\eta_{21} = \langle\varphi_2|\nabla\varphi_1\rangle = \nabla\theta$ is a vector, where $\langle ...\rangle$ indicates integration over the quantum coordinates. The component of the momentum parallel to the nonadiabatic coupling vector changes at each hop between adiabatic surfaces so that energy is conserved. The multisurface wave function, $\psi(\mathbf{R})$, is given by the sum of the contributions from all hopping and nonhopping trajectories that obey the appropriate initial conditions and end at $\mathbf{R}$. For instance, if the wave function describes colliding structureless particles with energy E, then the trajectories must have momentum $\mathbf{P}$ in the incoming region, where $\mathbf{P}$ is the appropriate relative momentum of the colliding particles. The transition amplitude in the multidimensional case is similar to that in the one-dimensional case given by eq 7, except that $d\theta/dX$ is replaced with the magnitude of $\nabla\theta$ multiplied by the sign of $\mathbf{P}_1\cdot\nabla\theta$, and the one-dimensional momenta P_1 and P_2 are replaced with the components of the vectors $\mathbf{P}_1$ and $\mathbf{P}_2$ parallel to η_{21}.

Every term in the one-dimensional surface hopping expansion diverges at turning points in the classical motion, because the prefactors have a $P^{-1/2}$ dependence. The divergence of the prefactor at a turning point (or a caustic in the multidimensioinal case) results in the usual semiclassical $-\pi/2$ addition to the phase.[6] An alternative uniform semiclassical surface hopping expansion of the wave function has recently been derived by generalizing the globally uniform single surface semiclassical wave function[7,8] to the multisurface case.[55] This global uniform wave function does not diverge at caustic points. It should be noted that, because these primitive and uniform semiclassical surface hopping wave function expansions are constructed using information gathered from classical trajectories, they cannot account for tunneling without additional features, as is commonly the case with semiclassical methods.

Numerical studies have shown that neglecting contributions involving the reflections with hops while keeping the contributions from transmission with hop terms generally results in very good accuracy.[22−25] The semiclassical and quantum transition probabilities are compared in Table 1 for a one-dimensional curve crossing problem.[22] The diabatic potential surfaces are shown in Figure 3. The initial state is the state with lower energy

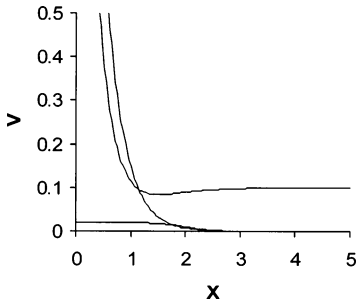

Figure 3. Diabatic potential energy surfaces $V_{11} = 3\exp(-3X)$, $V_{22} = 3\exp(-3X) - \exp(-2X) + 0.1$, and $V_{12} = 0.01\{1 - \tanh[2(X - 2)]\}$ are plotted.

TABLE 1: Comparison of Semiclassical (SC) and Quantum (Q) Transition Probabilities for the Model Problem Corresponding to the Diabatic Potential Energy Surfaces That Are Plotted in Figure 3

E (au)	p_{12}(SC)	p_{12}(Q)
0.25	0.981	0.953
0.50	0.661	0.659
0.75	0.391	0.389
1.00	0.130	0.131
1.50	0.764	0.765
2.00	0.032	0.032
3.00	0.576	0.575
5.00	0.00002	0.00002
10.0	0.079	0.079

at large X, and the other state is the final state. The semiclassical probabilities are evaluated using the primitive surface hopping expansion ignoring reflection with hop terms. The particle mass is taken to be the mass of a proton and atomic units are employed. The agreement between the semiclassical and quantum transition probabilities is excellent over the entire range of energies considered.

Only solutions to the TISE have been considered up to this point. A similar semiclassical surface hopping expansion can be developed that satisfies the time dependent Schrodinger equation (TDSE) to first order in $\hbar$ and all orders in the nonadiabatic coupling.[24] The propagator for the entire system becomes a matrix in the adiabatic state representation

$$K_{ab}(\mathbf{R}_1,\mathbf{R}_2,t) = \langle \varphi_a(\mathbf{r}_1,\mathbf{R}_2)|K(\mathbf{r}_1,\mathbf{R}_1,\mathbf{r}_2,\mathbf{R}_2,t)|\varphi_b(\mathbf{r}_2,\mathbf{R}_2)\rangle \tag{9}$$

where φ_a and φ_b are adiabatic quantum states, and $\langle ... \rangle$ indicates integration over the $\mathbf{r}_1$ and $\mathbf{r}_2$ quantum variables. The semiclassical surface hopping expansion[24] expresses $K_{ab}(\mathbf{R}_1,\mathbf{R}_2,t)$ as the sum of contributions from all energy conserving paths that start on surface a at $\mathbf{R}_1$ and end on surface b at $\mathbf{R}_2$ in time t. These paths can include any number of hops, and they obey the classical equations of motion between hops. As before, the component of the momentum parallel to the nonadiabatic coupling vector is altered at each hop to conserve energy. The zero hop contribution to $K_{aa}(\mathbf{R}_1,\mathbf{R}_2,t)$ is the well-known single surface semiclassical propagator,[1] and the expansion has a form analogous the surface hopping expansion for the time independent wave function.

As is the case with the propagator for single surface problems, the magnitude of the propagator diverges at caustics along the trajectory. It also shares with the single surface propagator the need to search for all trajectories that satisfy specific boundary conditions. In the multisurface case, this search is for all hopping and nonhopping trajectories that start at $\mathbf{R}_1$ and end at $\mathbf{R}_2$ at a time t later. These problematic issues can be avoided by casting the multisurface propagator as an initial value representation (IVR).[1,4,5,7] First, consider the single surface case. The primitive single surface propagator has the form

$$K(\mathbf{R}_1,\mathbf{R}_2,t) = \sum_j A_j e^{iS_j/\hbar} \tag{10}$$

where the sum is over all classical trajectories starting at $\mathbf{R}_1$ and ending at $\mathbf{R}_2$ at time t. The phase function is the classical action for the trajectory

$$S(\mathbf{R}_1,\mathbf{R}_2,t) = \int_0^t (T - V)\, dt_1 \tag{11}$$

where T is the kinetic energy and V is the potential energy. The prefactor A can be expressed as

$$A(\mathbf{R}_1,\mathbf{R}_2,t) = \left[(-2\pi i\hbar)^{-d}\left|\frac{\partial^2 S}{\partial \mathbf{R}_1 \partial \mathbf{R}_2}\right|\right]^{1/2} \tag{12}$$

Alternatively, the IVR version of the single surface propagator is expressed as a integration over the initial phase space point $\{\mathbf{R}_0, \mathbf{P}_0\}$ of the classical trajectories[1,4,5]

$$K^{IVR}(\mathbf{R}_1,\mathbf{R}_2,t) = \frac{1}{(2\pi\hbar)^d}\int d\mathbf{R}_0\, d\mathbf{P}_0\, g(\mathbf{R}_1;\mathbf{R}_0,\mathbf{P}_0)^* g(\mathbf{R}_2;\mathbf{R}_t,\mathbf{P}_1) C e^{iS/\hbar} \tag{13}$$

where d is the dimensionality of $\mathbf{R}$ and

$$g(\mathbf{R};\mathbf{R}_1,\mathbf{P}_t) = \left(\frac{2\gamma}{\pi}\right)^{d/4} \exp\left[-\gamma(\mathbf{R} - \mathbf{R}_t)^2 + \frac{i}{\hbar}\mathbf{P}_t\cdot(\mathbf{R} - \mathbf{R}_t)\right] \tag{14}$$

is a Gaussian function with average position $\mathbf{R}_t$ and average momentum $\mathbf{P}_t$. The constant γ determines the width of the Gaussian. The phase function S is again the classical action evaluated along the trajectory. The prefactor is given by[5]

$$C(\mathbf{R}_0,\mathbf{P}_0,t) = \left|\frac{1}{2}\left[\frac{\partial \mathbf{R}_t}{\partial \mathbf{R}_0} + \frac{\partial \mathbf{P}_t}{\partial \mathbf{P}_0} - 2i\gamma\hbar\frac{\partial \mathbf{R}_t}{\partial \mathbf{P}_0} - 2i\gamma\hbar\frac{\partial \mathbf{R}_t}{\partial \mathbf{P}_0} - \frac{1}{2i\gamma\hbar}\frac{\partial \mathbf{P}_t}{\partial \mathbf{R}_0}\right]\right|^{1/2} \tag{15}$$

Equation 13 expresses the time dependence of the propagator in terms of fixed width Gaussian functions that travel along classical trajectories. The specific IVR given by eqs 13−15 has been found to be a very useful semiclassical approximation to the full quantum propagator and is widely employed.

The generalization of the IVR propagator for multistate problems has the form[25]

$$K_{ab}^{IVR}(\mathbf{R}_1,\mathbf{R}_2,t) = K^{IVR,0}(\mathbf{R}_1,\mathbf{R}_2,t)\delta_{ab} + \sum_{n=1}^{\infty} K_{ab}^{IVR,n}(\mathbf{R}_1,\mathbf{R}_2,t) \tag{16}$$

where $K^{IVR,0}(\mathbf{R}_1,\mathbf{R}_2,t)$ is the single surface IVR propagator. The nth term in the summation in eq 16 contains contributions from trajectories with n hops between adiabatic surfaces. It is nth order in the nonadiabatic coupling. Neglecting reflection terms again, the first-order term is

$$K_{ab}^{IVR,1}(\mathbf{R}_1,\mathbf{R}_2,t) = \frac{1}{(2\pi\hbar)^d}\int d\mathbf{R}_0\, d\mathbf{P}_0 \int_0^t dt_1\, \tau_{ab}^{IVR}(t_1) g(\mathbf{R}_1;\mathbf{R}_0,\mathbf{P}_0)^* g(\mathbf{R}_2;\mathbf{R}_t,\mathbf{P}_t) C e^{iS/\hbar} \tag{17}$$

Equation 17 has a form similar to that of eq 13 with the addition of the integration over the time of the hop, t_1. Equation 17 expresses the first-order (in the nonadiabatic coupling) contribution to the propagator as an integration over the initial phase space points of single hop trajectories. Each trajectory evolves on the initial adiabatic surface, $W_a(\mathbf{R})$, according to the classical equations of motion until time t_1. At t_1, it undergoes a hop to $W_b(\mathbf{R})$ and then continues on this surface. The component of the momentum parallel to the nonadiabatic coupling vector changes so that the energy is unchanged by the hop. The hop also results in changes in the stability matrixes that appear in the prefactor, eq 15.[25,56] The amplitude for the hop at t_1 in eq 17 is given by[25]

$$\tau_{ab}^{\mathrm{IVR}}(t_1) = -\frac{(P_{a\eta} + P_{b\eta})}{2m}\eta_{ab}\,\mathrm{sgn}(\mathbf{P}_a\cdot\eta_{ab})\frac{C_a(t_1)}{C_b(t_1)} \quad (18)$$

where m is the mass, η_{ab} is the magnitude of the vector η_{ab} times the sign of $\mathbf{P}_a\cdot\eta_{ab}$, C_a is the value of the prefactor at t_1 before the hop, and C_b is its value at t_1 after the hop. This equation assumes a single mass in the problem. If this is not the case, then mass weighted coordinates can be employed.

The second-order term in the nonadiabatic IVR propagator contains the contributions from all trajectories with two hops. It has a form similar to that of eq 17 with a summation over all intermediates states c, integrations over the two hopping times, t_1 and t_2, with $0 < t_1 < t_2 < t$, and two transition amplitudes, one for the hop from state a to state c at t_1 and one for the hop from state c to state b at t_2. These transition amplitudes are given by eq 18. The nth-order term in eq 16 has summations over all possible sequences of the $n - 1$ intermediate states, integrations over the n hopping times, and n transition amplitudes.

III. Numerical Implementation

In this section, a Monte Carlo procedure is described to numerically implement the method discussed in the previous section.[25,57] Trajectories are started at some point X_i in the asymptotic incoming region on a chosen adiabatic potential energy surface with the appropriate initial momentum. The trajectories are divided into steps of length ΔX. At each step the contribution to the nonhopping trajectory is

$$a_{11} = \exp[(\mathrm{i}/\hbar)\textstyle\int_{X_j}^{X_{j=1}} P_1(y)\,\mathrm{d}y] \quad (19)$$

where the system is in quantum state one and X_j (X_{j+1}) is the point at the beginning (end) of the step. Here we allow for the possibility that $\Delta X = X_{j+1} - X_j$ is moderately large. In this case, the integral in eq 19 is evaluated numerically by taking a sufficient number of small substeps of width δX within the interval from X_j to X_{j+1} so that it can be accurately calculated. As is demonstrated below, the use of a relatively large ΔX can improve the numerical efficiency of the Monte Carlo procedure. The nonhopping term in the wave function, eq 4, is obtained by multiplying a_{11} by similar contributions from the other intervals and by the semiclassical prefactor.

The contribution to the one hop integral eq 5 in which the hop from surface one to surface two comes in the jth step is obtained by multiplying the hopping amplitude for the jth step

$$a_{21} = \textstyle\int_{X_j}^{X_{j+1}} \mathrm{d}y\,\tau_{12}(y)\exp[(\mathrm{i}/\hbar)\int_{X_j}^{y} P_1\,\mathrm{d}z + (\mathrm{i}/\hbar)\int_{y}^{X_{j+1}} P_2\,\mathrm{d}z] \quad (20)$$

by nonhopping amplitudes of the form of eq 19 from the other steps and by the semiclassical prefactor. These nonhopping and hopping amplitudes for the jth step, a_{11} and a_{21}, can be employed in a Monte Carlo procedure to decide whether the trajectory should hop in this step. The probability for staying on W_1 during the step is taken to be $p_1 = |a_{11}|/D_j$ and the probability for hopping to W_2 is taken to be $p_2 = |a_{21}|/D_j$, where $D_j = |a_{11}| + |a_{21}|$ so that $p_1 + p_2 = 1$. If a computer generated pseudo-random number ξ is smaller than p_1, then the trajectory stays on the same surface in this step. If $\xi \geq p_1$, then the trajectory hops in this step. In the discussion below, it is useful to express the amplitude associated with each outcome for the jth step, a_{11} or a_{21}, as the probability for that outcome multiplied by a modified amplitude c_j. Thus, $c_j = a_{21}/p_2 = D_j a_{21}/|a_{21}|$ if the hopping outcome is selected, and $c_j = a_{11}/p_1 = D_j a_{11}/|a_{11}|$ if it is not.

If the Monte Carlo procedure selects the option to hop during this step, then on the next step the amplitudes for staying on the same surface and for hopping back to W_1 are evaluated as in eqs 19 and 20 and p_1 and p_2 are defined as before, except that roles of the indices 1 and 2 are reversed and j is replaced by $j + 1$. The procedure is repeated for each step along the trajectory until a specified point in the final asymptotic region, X_f, is reached. The contribution from the trajectory is obtained by multiplying together the c_j factors from all steps. The contributions from all trajectories that end on each final surface W_f are averaged and the result is multiplied by the appropriate semiclassical prefactor $[P_1(X_i)/P_f(X_f)]^{1/2}$ to obtain the value of the wave function on W_f at X_f. Because this is a time independent stationary state problem, the probability of a particle coming in on W_1 and going out on W_f, where f can be 1 or 2, is given by the ratio of the outgoing flux and the incoming flux; i.e., $p_{1f} = |\psi_f(X_f)|^2 P_f(X_f)/|\psi_1(X_i)|^2 P_1(X_i)$. Notice that the P_f/P_1 factor in p_{1f} cancels the contribution from the wave function prefactors.

This method offers a potentially highly accurate procedure for obtaining transition probabilities. The contribution for each trajectory contains the product of the c_j factors. Because each c_j is proportional to D_j, the trajectory contribution is proportional to the product of the D_j

$$D = \prod_j D_j \quad (21)$$

If D can be much larger than 1, then there must be significant cancellation between trajectory contributions to obtain the correct value for the wave function. This cancellation can result in very large sampling errors in a Monte Carlo calculation with a fixed number of trajectories. In the remainder of this section, techniques are discussed that can dramatically improve the efficiency and reduce the statistical errors in Monte Carlo calculations of this type.

A. Improved Step Amplitudes. Consider the simple curve crossing problem with the diabatic potential surfaces $V_{11}^{\mathrm{d}} = \tanh(X)$, $V_{22}^{\mathrm{d}} = -V_{11}^{\mathrm{d}}$, and $V_{12}^{\mathrm{d}} = A_{12}\exp(-X^2/20)$. The surfaces V_{11}^{d} and V_{22}^{d} cross at $X = 0$. The nonadiabatic coupling is $\eta_{12} = \langle\varphi_2|\mathrm{d}\varphi_1/\mathrm{d}X\rangle = \mathrm{d}\theta/\mathrm{d}X$, and $\theta = {}^1/_2\tan^{-1}[2V_{12}^{\mathrm{d}}/(V_{11}^{\mathrm{d}} - V_{22}^{\mathrm{d}})]$. If the magnitude of the diabatic coupling V_{12}^{d} is relatively small near $X = 0$, η_{12} is sharply peaked at the crossing point with a width proportational to A_{12}. As A_{12} goes to zero, η_{12} approaches $(\pi/2)\delta(X)$, where $\delta(X)$ is the Dirac delta function. This shows that the nonadiabatic coupling is often very large near a point where the diabatic surfaces cross. If a large step size was used, then the probability for hopping would be very high. If this step was divided into two steps of half the size, then there would still be a relatively large Monte Carlo probability of a hop in each of the two smaller steps and there

would be a good probability that the Monte Carlo procedure would choose to hop to W_2 in the first step and back to W_1 in the second. This double hop option is not accounted for when the larger step size is employed, and a very small step size would have to be employed in the Monte Carlo method to obtain good results.

A useful variation on the Monte Carlo procedure is obtained by assuming the width of the step is sufficiently small that the *difference* in the phase integral for trajectories that hop at different points during the step is small and can be neglected. If the phase for all trajectories that hop during the step is evaluated as though all hops occur at the midpoint of the step, then the integrals corresponding to one, two, three, ... hops during the step can be performed analytically.[22,57,58] Summing contributions from all nonhopping, one hop, two hop, ... trajectories within this approximation, the amplitudes for the different possible outcomes during the interval are found to be $a_{jj} = \exp(iS_{jj}/\hbar)\cos(\gamma)$, $a_{21} = \exp(iS_{21}/\hbar)\sin(\gamma)$, and $a_{12} = -\exp(iS_{12}/\hbar)\sin(\gamma)$. The quantity γ is given by $\int \tau_{12}(y)\, dy$ and $S_{ij} = \int P(y)\, dy$, where the integrations are over the step and P is defined to be P_j (P_i) for first (second) half of the step. The Monte Carlo procedure can be performed as described above using these improved a_{ij}. Because these amplitudes include multihop contributions, they can provide accurate results with relatively large step sizes in regions of large coupling.

These improved amplitudes also have the appealing characteristic that the matrix

$$\mathbf{A} = \begin{pmatrix} a_{11} & a_{12} \\ a_{21} & a_{22} \end{pmatrix} \tag{22}$$

is unitary. This feature is lacking in the original amplitudes. If the incoming particle is on surface j, then the component of the wave function on surface k at the end of the Nth step is given by $m_{kj}[P_j(X_i)/P_k(X_N)]^{1/2}$, where m_{kj} is an element of

$$\mathbf{M} = \prod_{i=0}^{N} \mathbf{A}^{(i)} \tag{23}$$

and $\mathbf{A}^{(i)}$ is the $\mathbf{A}$ matrix for the ith interval. The probability that an incoming particle in state j will end in state k, p_{jk}, is given by the ratio of the outgoing and incoming fluxes, which yields the result

$$p_{jk} = |m_{kj}|^2 \tag{24}$$

If the $\mathbf{A}^{(i)}$ are unity, then $\mathbf{M}$ is unitary, and this guarantees that the sum of the probabilities for the possible outcomes, $p_{j1} + p_{j2}$, is equal to 1, and conservation of probability is guaranteed.

It should be noted that the simple matrix multiplication expression, eq 23, is only useful for one-dimensional problems, because multidimensional cases are complicated by the fact that the trajectories change direction at each hop. Therefore, the Monte Carlo procedure must be used for multidimensional problems. However, when various approximations on one-dimensional problems are tested, the matrix multiplication expression provides a very efficient way of exactly summing the contributions from all possible trajectories. The comparison of matrix multiplication results with exact quantum calculations allows for the determination of the ultimate accuracy of various semiclassical approximations, independent of statistical errors introduced by a Monte Carlo calculation.

The improved a_{ij} amplitudes for a single step, eqs 19 and 20, include the contributions from multihop terms. The phase factors in these amplitudes are evaluated under the approximation that all hops occur at the midpoint of the step. A better approximation can be developed as follows.[57,58] The general two-by-two unitary matrix can be expressed as

$$\mathbf{A} = e^{i\alpha/\hbar}\begin{pmatrix} e^{i\beta/\hbar}\cos(\gamma) & -e^{i\delta/\hbar}\sin(\gamma) \\ e^{i\delta/\hbar}\sin(\gamma) & e^{-i\beta/\hbar}\cos(\gamma) \end{pmatrix} \tag{25}$$

where α, β, γ, and δ are real constants. The higher order approximation is obtained by expressing the phase in the single hop, double hop, and higher hop integrals in the surface hopping expansion for the wave function as a zeroth-order approximation plus a correction term. The zeroth-order approximation treats all hops as occurring at the same point, X_h, and phase correction terms are treated as small. The exponentials of the phase correction terms are then expanded in a Taylor series. The parameters X_h, α, β, γ, and δ are chosen so that each element of eq 25 agrees with the exact result to third order in ΔX. If X_h is chosen so that the phases for a_{12} and a_{21} are the same as in the earlier model, then[57,58] $\alpha = (S_{11} + S_{22})/2$, $\delta = S_{12} - \alpha$,

$$\gamma = \int_{X_j}^{X_{j+1}} dy\, \tau_{12}(y) \cos\left(\frac{1}{\hbar}\int_{X_h}^{y} dz\, [P_2(z) - P_1(z)]\right) \tag{26}$$

and

$$\beta = (S_{11} - S_{22})/2 - \int_{X_j}^{X_{j+1}} dy\, \tau_{21}(y) \int_{y}^{X_{j+1}} dz\, \tau_{21}(z) \int_{y}^{z} ds\, [P_2(s) - P_1(s)] \tag{27}$$

The $P_2 - P_1$ terms in eqs 26 and 27 arise from the expansion of the phase correction terms.

This higher order expression for $\mathbf{A}$ has been tested on the one-dimensional two state model problem shown in Figure 1, where atomic units are employed and the particle has the mass of a proton.[57] At $E = 2.8$, the quantum transition probability for an incoming particle on lower surface ending on the upper surface is found to be $p_{12} = 0.640$. This quantum transition probability is evaluate using a Runge-Kutta method to integrate the two state Schrodinger equation. If a step size of $\Delta X = 0.1025$ is employed in the matrix multiplication method, as described by eqs 23 and 24, the semiclassical surface hopping method gives $p_{12} = 0.659$ if the simple form of the $\mathbf{A}$ matrix, eqs 19 and 20, is employed and $p_{12} = 0.641$ if the higher order form is used.[57] If a step size is doubled to $\Delta X = 0.205$, then the higher order $\mathbf{A}$ yields $p_{12} = 0.651$, which is still of higher accuracy than the results using the lower order $\mathbf{A}$ and the smaller step size.

If the Monte Carlo method described above had been used in the calculations, then each trajectory would be multiplied by the factor of D, eq 21. The larger the value of D, the more cancellation there must be between contributions from different trajectories to arrive at the correct value of p_{12}. The value of D for the calculation using the higher order $\mathbf{A}$ and $\Delta X = 0.205$ is $D = 4.86$, and the value of D when the lower order $\mathbf{A}$ is employed and $\Delta X = 0.1025$ is $D = 9.86$.[57] Because D is about twice as large in the latter case, the relative statistical error in a Monte Carlo calculation of the wave function would have to be roughly half as great as it is in the higher order calculation to obtain a comparably accurate result. Assuming that the relative statistical error has a $N_{tr}^{-1/2}$ dependence on the number of trajectories sampled, then the use of the higher order $\mathbf{A}$ matrix is expected to cut the number of trajectories needed to achieve a desired accuracy by about a factor of 4.

B. Selecting a Good Representation of the Quantum States. An adiabatic representation of the quantum states of the

TABLE 2: Value of G and Semiclassical p_{12} for the Adiabatic (A), Diabatic (D), and Optimal (O) Representations for Curve Crossing Problem[a]

E	G (A)	G(D)	G(O)	G(AO)	p_{12}(A)	p_{12}(D)	p_{12}(O)	p_{12}(Q)
1.3	1.57	24.8	1.24	1.20	0.43	0.43	0.44	0.43
2.0	1.57	18.0	1.12	1.10	0.51	0.51	0.51	0.51
5.0	1.57	10.9	0.90	0.90	0.65	0.65	0.65	0.65
10.0	1.57	7.64	0.76	0.76	0.74	0.74	0.74	0.74
20.0	1.57	5.40	0.64	0.66	0.81	0.81	0.81	0.81
40.0	1.57	3.82	0.54	0.56	0.86	0.86	0.86	0.86
100.0	1.57	2.42	0.44	0.46	0.91	0.91	0.91	0.91
200.0	1.57	1.70	0.38	0.40	0.93	0.93	0.93	0.93

[a] The quantum (Q) p_{12} is given for comparison. The value of G for the approximate optimal (AO) representation is also given.

fast subsystem has been employed in the development of the nonadiabatic semiclassical surface hopping wave functions and propagators up to this point. The adiabatic representation of the quantum states has the property that it diagonalizes the matrix $V_{if} = \langle\varphi_i|\mathbf{H}^f|\varphi_j\rangle$, where $\mathbf{H}^f$ is the Hamiltonian for the fast subsystem. The diabatic representation, on the other hand, is defined such that the kinetic energy operator for the slow subsystem is diagonal. In this case, V_{if} is no longer diagonal. It is also possible to choose a representation that is neither adiabatic nor diabatic. In a two state problem, this general representation can still be defined in terms of the diabatic states by eq 3, but without requiring that $\theta(\mathbf{R})$ be chosen so that $\langle\varphi_i|\mathbf{H}^f|\varphi_j\rangle$ is diagonal at each $\mathbf{R}$. The flexibility in the choice of $\theta(\mathbf{R})$ can be used to improve the efficiency of the Monte Carlo calculations. The semiclassical surface hopping wave function or propagator can be modified to allow for a general representation.[59] The expressions for the propagator and wave function remain as before, except that the nonadiabatic coupling, η_{if}, is replaced with

$$s_{if} = \eta_{if} + imV_{if}/(2\hbar P_i) \tag{28}$$

In this expresion, V_{if} and $\eta_{if} = \langle\varphi_f|\nabla\varphi_i\rangle$ depend on the representation chosen. The energy conserving change in momentum at a hop is required to be in the direction parallel to η_{if}.

Once the semiclassical surface hopping wave function and propagator have been defined for a general representation, the flexibility in the choice of the representation can be utilized to reduce the average number of hops along a trajectory in the Monte Carlo procedure. This is accomplished by choosing the angle θ at each point along the trajectory so as to minimize the integral of the magnitude of the coupling, $|s_{if}|$, where this integral is taken over the entire trajectory. The actual integral minimized in calculations is[59]

$$G = \int_{-\infty}^{\infty}\left[\eta_{if}^{\ 2} + \frac{m^2V_{if}^{\ 2}}{\hbar^2P_iP_f}\right]^{1/2} \mathrm{d}X \tag{29}$$

The P_iP_f factor in the denominator is employed because a hop from W_i to W_f would have a factor of P_i^2 whereas a hop from W_f to W_i would have a factor of P_f^2. Equation 29 accounts for hops in both directions.

Consider the simple curve crossing example with $V_{11}^d = -V_{22}^d = \tanh(X)$, $V_{12}^d = \exp(-X^2/20)$, and $m = 1836.2$ au. Results for G for the adiabatic, diabatic, and optimal representations are reported in Table 2 for different values of E.[59] The value of G for the diabatic and optimal representations depends on E through the P_iP_f factor in eq 29. The result for the adiabatic representation is independent of E, because $V_{12} = 0$ in this case. For the model considered here with a single crossing of V_{11}^d and V_{22}^d, $G = \pi/2$ in the adiabatic representation at all E. G becomes smaller as E increases for both the diabatic representation and the optimal representation, reflecting the fact that the diabatic representation provides a better description of the curve crossing dynamics at higher energies (faster collisions). At $E = 1.3$, the optimal representation gives a G that is about a factor of 0.8 times the G for the adiabatic representation. Thus, single hop trajectories are roughly 0.8 times as likely if the optimal representation is employed than if the adiabatic representation is used. One would expect n-hop trajectories to be roughly $(0.8)^n$ times as likely in the optimal representation. Thus, one would expect a significant reduction in the importance of multihop trajectories when optimal representation is employed. As E increases, the reduction in G obtained by using the optimal representation is more pronounced. At $E = 40$, the value of G for the optimal representation is about one-third its value for the adiabatic representation. Table 2 also presents results for the transition probability for a particle coming in on the lower adiabatic surface and ending on the upper adiabatic surface.[59] The quantum transition probabilities are again calculated using a Rugge-Kutta integration. The data confirm that the semiclassical surface hopping method accurately reproduces the quantum transition probability in all representations considered.

The method just described involves a nonlocal optimization of $\theta(X)$. This was numerically accomplished by choosing a set of equally spaced points on the X axis, X_0, X_1, X_2, ..., X_N, and replacing the integral in eq 29 with a finite difference approximation.[59] This discretized G depends on the value of θ at each of the X points. The problem is then a multivariable minimization problem. The results from calculations[59] show that the $\theta(X)$, $W_1(X)$, and $W_2(X)$ for the optimal representation are essentially the same as for the adiabatic representation when $|X| \gg 0$. However, as X approaches the crossing point at zero, the representation crosses over to the diabatic representation (i.e., $\theta = 0$). The optimal representation is close to the adiabatic representation at large $|X|$, because the coupling in the adiabatic representation is smaller in this region than in the diabatic representation. However, the adiabatic coupling $\eta_{if}^{ad} = \mathrm{d}\theta^{ad}/\mathrm{d}X$ becomes large at small $|X|$, and the optimal representation avoids this large coupling by switching over to the diabatic representation as X goes to zero.

The sharpness of the crossover depends on the energy and the X dependence of V_{12}^d, V_{11}^d, and V_{22}^d in the region near the crossing point. A simpler numerical approach is to use an analytical switching function to have $\theta(X)$ cross over from $\theta^{ad}(X)$ far from the crossing point to $\theta = 0$ at the crossing point. A hyperbolic tangent function, $f(X) = |\tanh(X/w)|$, is an example of a simple crossover function that has been employed in numerical studies.[59] In these studies, the value of the crossover width w is estimated at each point along the trajectory by taking w to be the value that is optimal for the corresponding Landau−Zener[60,61] (i.e., constant V_{12} and constant $\mathrm{d}V_{11}/\mathrm{d}x - \mathrm{d}V_{22}/\mathrm{d}x$) problem. In this approach, w is X dependent. The representation obtained by this procedure is referred to as the approximation optimal representation (AOR). The data presented in Table 2 show that the value of G obtained when the AOR is employed is not significantly higher than the G for the optimal representation (OR). (The slightly higher value of G for the OR at low E, compared with the AOR, results from incomplete convergence of the minimization problem involved in obtaining the OR.)

Figure 4 presents results[57] for the transition probability p_{12} as a function of energy for the two crossing point model shown in Figure 1. The solid line is the quantum transition probability

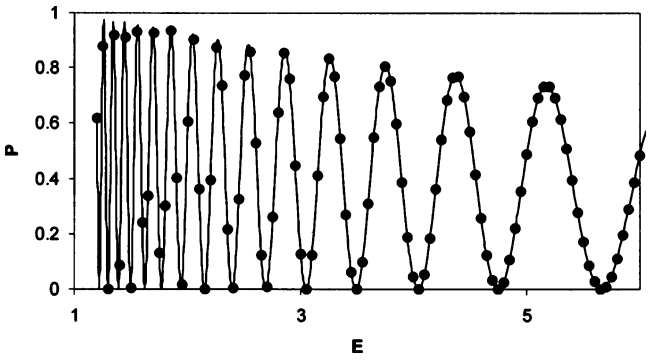

Figure 4. Quantum (solid line) and semiclassical (dots) transition probabilities are plotted as a function of energy for the model problem corresponding to diabatic potential surfaces shown in Figure 1.

TABLE 3: Semiclassical Results for Curve Crossing Problem in Figure 1 at $E = 2.8$[a]

representation	A	ΔX	p_{MM}	p_{MC}	σ	D	⟨hops⟩
adiabatic	lower order	0.005125	0.640	0.475	0.235	19.9	2.97
adiabatic	lower order	0.05125	0.645	0.745	0.213	13.7	2.65
adiabatic	lower order	0.1025	0.659	0.605	0.103	9.86	2.47
adiabatic	higher order	0.1025	0.641	0.569	0.086	8.88	2.36
adiabatic	higher order	0.205	0.651	0.619	0.045	4.86	1.95
AOR	lower order	0.005125	0.637	0.594	0.041	4.87	1.57
AOR	lower order	0.1025	0.638	0.649	0.031	4.06	1.43
AOR	higher order	0.1025	0.636	0.644	0.029	3.78	1.36
AOR	higher order	0.205	0.635	0.661	0.022	2.97	1.14

[a] p_{MM} is matrix multiplication p_{12}. p_{MC} is the value of p_{12} from a 10 000 trajectory Monte Carlo calculation, and σ is the estimated Monte Carlo statistical error. See text for definition of other quantities.

and the dots are semiclassical surface hopping transition probabilities obtained using the matrix multiplication method with $\Delta X = 0.005\,125$. The oscillations in the transition probability result from the interference between trajectories that hop between surfaces near the first crossing point and those that hop between surfaces near the second crossing point. The semiclassical surface hopping procedure clearly provides very high accuracy results at all energies, and it accurately accounts for the phase interference between the various hopping trajectories.

Table 3 provides data on the accuracy of various calculations using either the lower order **A** matrix or the higher order **A** matrix, using either the adiabatic representation or the AOR, and using different values of ΔX.[57] The results demonstrate that for a given level of approximation for **A** and for a fixed value of ΔX, the use of the AOR significantly reduced the value of D while maintaining similar accuracy. For example, when the lower order **A** is employed and $\Delta X = 0.05125$, $D = 13.7$ if the adiabatic representation is used and $D = 4.87$ if the AOR is used. If the higher order **A** is utilized and $\Delta X = 0.1025$, then $D = 8.88$ using the adiabatic representation and $D = 3.78$ when the AOR is employed. These reductions in D are expected to result in a significant improvement in the efficiency of the Monte Carlo method due to a large reduction in the number of trajectories that are needed to obtain a desired level of statistical accuracy. All of the calculations just mentioned yield highly accurate transition probabilities by the matrix multiplication method. If the higher order **A** and the AOR are used, then $\Delta X = 0.205$ can be employed without loss of accuracy. In this case, $D = 2.97$. Thus, there is an overall reduction in D from 13.7 to 2.97 without loss of accuracy by increasing the order of **A** and using the AOR. Matrix multiplication calculations using the higher order **A**, the AOR, and $\Delta X = 0.205$ provide energy dependent results for which the agreement with the quantum results is are not noticeably different from that shown in Figure 4.[57]

The statistical accuracy of Monte Carlo calculations at $E = 2.8$ using the semiclassical surface hopping procedure is also considered in Table 3.[57] A sample of 10 000 trajectories is used in each calculation. The statistical error σ is estimated for each calculation by dividing the sample into $N_s = 100$ subsamples of 100 trajectories each. The error is then obtained as the root-mean-squared deviation of the subaverages divided by square root of $N_s - 1$. This analysis assumes that the statistical errors in the Monte Carlo calculations scale as $1/N_{tr}^{1/2}$, where N_{tr} is the number of trajectories in the sample. This dependence has been verified numerically. If the calculations are run with 100 subsamples of 1000 trajectories each, then the calculated errors are about $1/10^{1/2}$ smaller than the errors shown in Table 3. For example, when this larger calculation is performed for the case where $\Delta X = 0.1025$, the AOR is used, and the higher order **A** is employed, then the calculated σ is 0.0089, as compared with 0.029 for the corresponding calculation shown in Table 3. As is clear from the data in Table 3, much larger trajectory samples than those employed here are necessary to obtain accurate transition probabilities when D is relatively large, whereas the statistical errors are quite small $\sigma \approx 0.02$ for the calculations with small values of D. It is interesting to compare the results for the basic calculation (i.e., lower order **A**, adiabatic representation) with $\Delta X = 0.05125$ with those for the most refined calculation (i.e., higher order **A**, AOR) with $\Delta X = 0.205$, because these have similar accuracies when the matrix multiplication method is employed. It is found that the latter calculation shows a 10-fold improvement in the statistical error over the former. Because $\sigma \sim 1/N_{tr}^{1/2}$, it is expected that a calculation of around 1 000 000 trajectories would be required to obtain the same level of accuracy using the basic method as is obtained using the most refined calculation in a 10 000 trajectory calculation. A detailed analysis of the statistics of the problem[57] shows that the statistical error in the most refined calculations reported in Table 3 is mainly due to fluctuations in the number of trajectories ending in each state, rather than from an inability to accurately account for the phase cancellation between the trajectories ending in a given state.

The results obtained for this two state problem with two curve crossing points have also obtained employing the widely used Tully's fewest switches (TFS) method.[57] It is found that the fewest switches model does not accurately account for the interference between hopping trajectories, and this results in inaccurate results for this problem. On the other hand, the statistical errors in the TFS results are significantly smaller than those found in even the most refined calculations considered in Table 3. The reason for this is that the TFS approach provides transition amplitudes for both surfaces, independent of the surface on which the trajectory ends, whereas the surface hopping method discussed in this work provides a nonzero amplitude only for the final surface for the trajectory and a zero amplitude for the other surface. This results in a smaller fluctuation in the value of the amplitudes from trajectory to trajectory for the TFS method.

Table 3 also includes the average number of hops per trajectory for each calculation. As expected, increasing the size of ΔX decreases the average number of hops, because multihop contributions within a single step become more important and these are incorporated into the amplitude for hopping or not hopping during the step. The average number of hops per

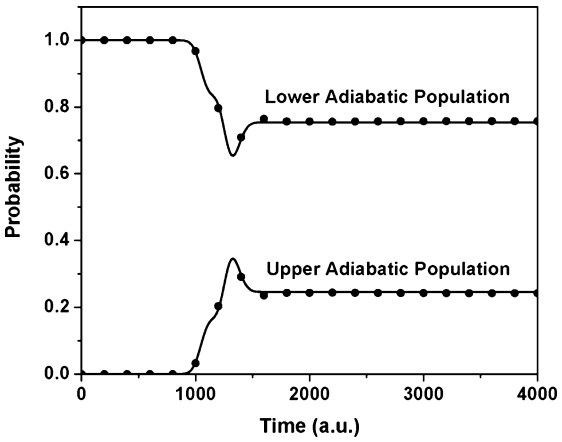

Figure 5. Comparison of the time dependent quantum (solid line) and semiclassical probabilities[62] (dots) that the particle is on the upper and lower adiabatic surfaces for Tully's dual crossing model.[57] The initial wave function is a Gaussian wave packet centered at $X_0 = -15.0$ on lower adiabatic surface with an average momentum of $P_0 = 25.0$, particle mass of 2000 au, and a width parameter of $\gamma = P_0^2/400$ [see eq 14]. The semiclassical probabilities are evaluated using the surface hopping IVR propagator, eq 16.

trajectory also decreases when going from the adiabatic to the approximate optimal representation, as anticipated.

IV. Concluding Remarks

The goal of the work described is the development of an accurate and efficient semiclassical surface hopping method for nonadiabatic problems. Starting from a formally exact surface hopping expansion of the time independent wave function with the WKB approximation as the zeroth-order term, it is possible to obtain semiclassical surface hopping wave functions and propagators for multistate problems in many dimensions. Both primitive and uniform expressions have been obtained for the time independent and the time dependent cases. Results for model problems show that the method provides excellent results, even in cases where it is essential to accurately account for interference between trajectories that hop multiple times and at different hopping points. A Monte Carlo implementation of the surface hopping method is usually necessary for multidimensional problems, and the cancellation that occurs between contributions from different trajectories can lead to large Monte Carlo statistical errors. This "sign problem" is a common difficulty in quantum and semiclassical methods. Results shown here demonstrate that this numerical problem can be significantly reduced through the use of higher order amplitudes for hopping and nonhopping paths during each step along the trajectory, and by taking advantage of the flexibility in the choice of the representation of the quantum states for the fast degrees of freedom to minimize the integrated coupling between the states.

The numerical data presented are restricted to one-dimensional time independent model problems. Monte Carlo calculations using the surface hopping method have also been performed for one and two-dimensional time dependent problems, yielding very accurate results.[25,62,63] An example is shown in Figure 5. Future work will focus on the extension of the techniques to improve the efficiency of the Monte Carlo calculations discussed here to time dependent and multidimensional problems. Multidimensional problems have the added feature that they require a Monte Carlo selection of the initial conditions for trajectories. This phase space sampling can contribute to the sign problem. Various integral conditioning techniques have been employed to reduce the phase interference problems for single surface Monte Carlo calculations.[64−67] It will, in all likelihood, be important to use all of these techniques in tandem to obtain a generally accurate and efficient semiclassical surface hopping method for multidimensional problems.

Acknowledgment. This work is supported by NSF grant CHE-0203041. I am indebted to Feng Ding, Ouafae El Akramine, Michael P. Moody, and Yinghua Wu for their efforts and insight on the work described in this article.

References and Notes

(1) Miller, W. H. *Adv. Chem. Phys.* **1974**, *25*, 69; **1975**, *30*, 77.
(2) Marcus, R. A. *J. Chem. Phys.* **1971**, *54*, 3965; **1972**, *56*, 311; **1973**, *59*, 5135.
(3) Heller, E. J. *J. Chem. Phys.* **1975**, *62*, 1544; **1981**, *75*, 2923; **1991**, *94*, 2723.
(4) Herman, M. F.; Kluk, E. *Chem. Phys*. **1984**, *91*, 27.
(5) Kluk, E.; Herman, M. F.; Davis, H. L. *J. Chem. Phys.* **1986**, *84*, 326.
(6) Child, M. S. *Semiclassical Mechanics with Molecular Applications*; Clarendon: Oxford, 1991.
(7) Kay, K. G. *J. Chem. Phys.* **1994**, *100*, 4377, 4432; **1994**, *101*, 2250.
(8) Zor, D.; Kay, K. G. *Phys. Rev. Lett.* **1996**, *76*, 1990.
(9) Madhusoodanan, M.; Kay, K. G. *J. Chem. Phys*. **1998**, *109*, 2644.
(10) Makri, N.; Miller, W. H. *J. Chem. Phys.* **2002**, *116*, 9207.
(11) Wang, H.; Sun, X.; Miller, W. H. *J. Chem. Phys*. **1998**, *108*, 9726.
(12) Sun, X. Wang, H.; Miller, W. H. *J. Chem. Phys*. **1998**, *109*, 4190.
(13) Levine, I. N. *Quantum Chemistry*, 5th ed.; Prentice Hall, Upper Saddle River, NJ, 2000.
(14) Delos, J. B.; Thorson, W. R.; Knudson, S. K. *Phys. Rev. A* **1972**, *6*, 709.
(15) Delos, J. B.; Thorson, W. R. *Phys, Rev. A* **1972**, *6*, 720.
(16) Billing, G. D.; Jolicard, G. *Chem. Phys.* **1982**, *65*, 323.
(17) De Pristo, A. E. *J. Chem. Phys*. **1983**, *78*, 1237.
(18) Billing, G. D. *J. Chem. Phys*. **1993**, *99*, 5849.
(19) Pechukas, P. *Phys. Rev.* **1969**, *181*, 166, 174.
(20) Preston, R. K.; Tully, J. C. *J. Chem. Phys.* **1971**, *54*, 4297.
(21) Tully, J. C.; Preston, R. K. *J. Chem. Phys.* **1971**, *55*, 562.
(22) Herman, M. F. *J. Chem. Phys*. **1982**, *76*, 2949.
(23) Herman, M. F. *J. Chem. Phys*. **1984**, *81*, 754.
(24) Herman, M. F. *J. Chem. Phys*. **1985**, *82*, 3666; **1995**, *103*, 8081.
(25) Yang, G.; Herman, M. F. *J. Phys. Chem. B* **2001**, *105*, 6562.
(26) Tully, J. C. *J. Chem. Phys*. **1990**, *93*, 1061.
(27) Hammes-Schiffer, S.; Tully, J. C. *J. Chem. Phys*. **1994**, *101*, 4657.
(28) Sholl, D., S.; Tully, J. C. *J. Chem. Phys*. **1998**, *109*, 7702.
(29) Fang, F.-Y.; Hammes-Shiffer, S. *J. Chem. Phys*. **1997**, *107*, 8933; **1999**, *110*, 11166.
(30) Burant, J. C.; Tully, J. C. *J. Chem. Phys*. **2000**, *112*, 6097.
(31) Webster, F.; Wang, E. T.; Rossky, P. J.; Friesner, R. A. *J. Chem. Phys*. **1994**, *100*, 4847.
(32) Bittner, E. R.; Rossky, P. J. *J. Chem. Phys*. **1995**, *103*, 8130; **1997**, *107*, 8611.
(33) Ben-Nun, M.; Martinez, T. J. *J. Chem. Phys*. **1998**, *108*, 7244.
(34) Volobuev, Y. L.; Hack, M. D.; Topaler, M. S.; Truhlar, D. G. *J. Chem. Phys*. **2000**, *112*, 9716.
(35) Topaler, M. S.; Allison, T. C.; Schwenke, D. W.; Truhlar, D. G. *J. Phys. Chem. A* **1998**, *102*, 1666.
(36) Hack, M. D.; Wensmann, A. M.; Truhlar, D. G.; Ben-Nun, M.; Martinez, T. J. *J. Chem. Phys*. **2001**, *115*, 1172.
(37) Jasper, A. W.; Hack, M. D.; Truhlar, D. G. *J. Chem. Phys*. **2001**, *115*, 1804.
(38) Jasper, A. W.; Stechmann, S. N.; Truhlar, D. G. *J. Chem. Phys*. **2002**, *116*, 5424.
(39) Jasper, A. W.; Truhlar, D. G. *Chem. Phys. Lett*. **2003**, *369*, 60.
(40) Nangia, S.; Jasper, A. W.; Miller, T. F., III; Truhlar, D. G. *J. Chem. Phys*. **2004**, *120*, 3586.
(41) Zhu, C.; Kamisaka, H.; Nakamura, H. *J. Chem. Phys*. **2002**, *116*, 2324.
(42) Kondorshiy, A.; Nakamura, H. *J. Chem. Phys*. **2004**, *120*, 8937.
(43) Meyer, H.-D.; Miller, W. H. *J. Chem. Phys*. **1979**, *70*, 3214.
(44) Muller, U.; Stock, G. *J. Chem. Phys*. **1998**, *108*, 7516.
(45) Stock, G.; Thoss, M. *Phys. Rev. A* **1999**, *59*, 64.
(46) Bonella, S.; Coker, D. F. *J. Chem. Phys*. **2001**, *114*, 7778; **2003**, *118*, 4370.
(47) Sun, X.; Miller, W. H. *J. Chem. Phys.* **1997**, *106*, 6346.
(48) Sun, X.; Wang, H.; Miller, W. H. *J. Chem. Phys*. **1998**, *109*, 7064.
(49) Coker, D. F.; Xiao, L. *J. Chem. Phys*. **1995**, *102*, 496.
(50) Wan, C. C.; Schofield, J. *J. Chem. Phys.* **2000**, *113*, 7047.

(51) Nielsen, S.; Kapral, R.; Ciccotti, G. *J. Chem. Phys*. **2000**, *112*, 6543.
(52) Kernan, D. M.; Ciccotti, G.; Kapral, R. *J. Chem. Phys*. **2002**, *116*, 2346.
(53) Krylov, A. I.; Gerber, R. B.; Coalson, R. D. *J. Chem. Phys*. **1996**, *105*, 4626.
(54) Miller, W. H.; George, T. F. *J. Chem. Phys*. **1972**, *56*, 5637.
(55) Herman, M. F.; El Akramine, O.; Moody, M. P. *J. Chem. Phys.* **2004**, *120*, 7383.
(56) The ratio of the prefactors in eq 18 was left off in the corresponding equation in ref 25.
(57) Herman, M. F.; Moody, M. P. *J. Chem. Phys.* **2005**, *122*, 94194.
(58) Moody, M. P.; Ding, F.; Herman, M. F. *J. Chem. Phys.* **2003**, *119*, 11048.
(59) Herman, M. F. *J. Chem. Phys.* **1999**, *110*, 4141; **1999**, *111*, 10427.
(60) Landau, L. D. *Phys. Z. Sowjetunion* **1932**, *2*, 46.
(61) Zener, C. *Proc. R. Soc. London, Ser. A* **1932**, *137*, 696.
(62) Wu, Y. Herman, M. F., manuscript in preparation.
(63) Wu, Y.; Herman, M. F.; Batista, V. S. *J. Chem. Phys.* **2005**, *122*, 114114.
(64) Herman, M. F. *Chem. Phys. Lett.* **1997**, *275*, 445.
(65) Guerin, B. E.; Herman, M. F. *Chem. Phys. Lett.* **1998**, *286*, 361.
(66) Walton, A. R.; Manolopoulos, D. E. *Mol. Phys.* **1995**, *87*, 961.
(67) Wang, H.; Manolopoulos, D. E. *J. Chem. Phys.* **2001**, *115*, 6317.